MRS Advances (2025) 10:1103–1108
https://doi.org/10.1557/s43580-025-01284-x

ORIGINAL PAPER

Effect of post-heat treatment on mechanical, microstructure, and thermal properties of Nitinol (NiTiNb) manufactured using laser direct metal deposition (LDMD) process

Samuel Skhosane[1,2] · Nthabiseng Maledi[2] · Sisa Pityana[1,4] · Paul Lekoadi[1] · Monnamme Tlotleng[1,3]

Received: 29 January 2025 / Accepted: 1 May 2025 / Published online: 15 May 2025

Abstract

This study investigated the effect of annealing on the microstructure, mechanical properties, and thermal properties of $Ti_{51.25}Ni_{41.25}Nb_{7.5}$ ternary nitinol alloy manufactured using the laser direct metal deposition (LDMD) technique. The mechanically pre-alloyed powder consisting of the composition of $Ti_{52.5}Ni_{42.5}Nb_{7.5}$ was used as a feedstock to manufacture cubic samples on a Ti6Al4V base plate. The manufactured samples were subjected to post-heat treatment at temperatures of 700 °C and 900 °C. The produced samples were then characterized using scanning electron microscope (SEM), Vickers hardness, nano-indentation, Differential Scanning Calorimeter (DSC), and X-ray diffraction (XRD). SEM micrographs of both annealed samples showed dissolution of the eutectic phase that was present in the as-built sample into the matrix as β-Nb phase, which resulted in the annealed samples having increased hysteresis. The Ni_3Ti peaks' prominence increased with annealing temperature, leading to an increase in hardness.

Introduction

Nickel (Ni) and titanium (Ti) binary alloy, also known as Nitinol (NiTi) alloy, is produced at approximately equal atomic percent of pure Ni and pure Ti. This combination has special properties, such as superelasticity, shape memory effect, low stiffness, and good corrosion resistance [1, 2]. In 1959, Scientist, Buehler W.J., discovered the shape memory effect of NiTi when heating a folded strip of NiTi. [3], since then there has been industrial applications in the aerospace and medical fields for this alloy. In the aerospace sector, nitinol alloy is used for the manufacture of aircraft thermo-power actuators and thermomechanical connectors, and within the medical field, it is used as constrictive stents and implants [4]. The use of nitinol material for manufacturing implants and stents has surpassed the use of stainless steel because nitinol has good biocompatibility and low elastic properties [5].

The most common manufacturing process used to produce nitinol implants and stents is still the casting or powder metallurgy process, also known as the sintering process. However, both these processes have limitations. For instance, the production of nitinol via vacuum arc melting requires an inert atmosphere to avoid oxidation, and in addition, the use of crucibles to cast is likely to contaminate the final product, which can impact the mechanical properties. Also, the casting process involves multiple steps, which include melting, alloying, casting, and removal of unwanted material (pouring and risers) before the final part can be machined, work hardened, and annealed, which is time-consuming. On the other hand, the sintering process requires a higher temperature, which attracts the formation of impurities [6]. Moreover, these processes have limitations in fabricating complex parts [7]. The as-cast NiTi components manufactured for biomedical applications have an elastic modulus ranging from 28–41 GPa for the B19 martensitic phase and

✉ Samuel Skhosane
sskhosane@csir.co.za

1 Council for Scientific and Industrial Research, Manufacturing, Photonics Centre, Laser Enabled Manufacturing Group, P.O. Box 395, Pretoria 0001, South Africa

2 School of Chemical and Metallurgical Engineering, University of the Witwatersrand, Private Bag 3, Wits, Johannesburg 2050, South Africa

3 Material Science Innovation and Modelling Research Group, North-West University, Mahikeng Campus, Mmabatho, South Africa

4 Department of Chemical, Metallurgical and Material Engineering, Tshwane University of Technology, Staatsartillerie Road, Pretoria West, Pretoria, South Africa

41–75 GPa for the B2 austenitic phase.This is slightly higher than the elastic modulus for human bones measured using ultrasonic testing, which ranges between 10 and 30 GPa [8, 9]. Current research proposes that nitinol samples can be enhanced or improved by adding third metallic elements to the binary balanced Ti–Ni alloy to form a ternary NiTi alloy [10, 11]. Commonly known elements are niobium (Nb), iron (Fe), and copper (Cu), and among these elements, Nb is one of the promising additions since it has good biocompatibility and it enhances mechanical properties. However, minor additions have yielded an increase in hardness due to the interstitial hardening effect [11, 12], while excess additions of Nb yield segregation of β-Nb-rich, with a eutectic structure; therefore, a balance must be attained.

Ying et al. [12] observed that microalloying of nickel-rich NiTi alloy with 3.5 wt% and 5 wt% Nb, respectively, improved the yield strength and ductility, thus making it easier for machining. Nb also serves as a lubricant in nitinol alloy, where it forms the Nb_2O_5 phase that improves the surface wear resistance [11, 13]. In addition, Nb improves the hysteresis of NiTi samples [14], and copper (Cu) does not [12, 15–17]. It was observed that less or more of Nb added leads to the reduction in the shape memory effects because of the irreversible plasticity of Nb [13], and that ultimately, when fabricated using arc melting, the NbNiTi sample transformation temperature increases when the ratio of Ni: Ti ($\geq$) is greater or equal to 1; otherwise, the M_S temperature is reduced when Ni:Ti ratio is less or equalling ($\leq$) to 1 [18, 19]. However, Zhu et al. [7] found that $Ni_{47}Ti_{44}Nb_9$ plate produced via induction arc melting and then hot worked at 850 °C yields a significant improvement in the recovery rate.

Heat treatment has a positive influence on the resulting microstructure; it reduces residual stresses, brings about the homogenization of precipitation, and eventually enhances the mechanical properties, including superelasticity and shape memory behavior [6]. Moreover, aging tremendously impacts the superelasticity of NiTi alloys even at short durations [17], and over prolonged time, it can somewhat diminish. Precisely, the shape memory and superelasticity of a deformed nitinol binary system (Ni–Ti) can be recovered by aging at temperatures ranging from 500 to 550 °C. Halani et al. [6] also found that annealing of nickel-rich nitinol at 1050 °C reduces the martensitic start temperature to below − 60 °C.

While cast and heat-treated NiTi parts are promising, the challenge is in producing complex parts. Additive Manufacturing (AM), a group of manufacturing techniques including direct energy deposition (DED) and selective laser melting (SLM), seems to be gradually getting traction within the manufacturing industries globally. AM process is popular in fabricating complex shape parts, such as those found in the biomedical field, layer-by-layer [20–22]. However, fabrication of implants using the AM process yields higher hardness than the as-cast due to the fast cooling [11, 14], leading to difficulties in machining and high wear on tools. To fabricate industrial stents using AM, it is proposed that during manufacturing, laser energy density must be reduced [23]. Unalloyed nickel-rich nitinol ($Ni_{55}Ti_{45}$) produced via the SLM system has a higher hardness [16], making this alloy prone to cracking and difficult to machine. Polozov et al. [4] showed that a ternary NiTiNb sample produced via SLM has an increased Hysteresis, while Zhang et al. [24] showed that the annealing of NiTiNb alloy increases both the hardness and tensile strength. Xi et al. [25] investigated the effect of solution heat treatment at 1273 K on microstructure and functional properties of NiTiNb fabricated via laser powder bed fusion, and the results showed distributed precipitates and coarsened β-Nb phase, which improved tensile strength. Moreover, hysteresis was not affected by the holding time.

While it is evident from the literature that adding Nb on Ni/Ti ratio ≤ 1 reduces the Ms temperature, and that annealing significantly improves hysteresis, there is still a gap in studies that report the effects of annealing the Ti–rich ternary nitinol alloy that is micro-alloyed with Nb and produced using DED techniques. In this study, the investigation focused on studying the influence of annealing on the microstructure, mechanical, and thermal properties of Ti–rich nitinol that contained Nb ($Ti_{51\cdot25}Ni_{41.25}Nb_{7.5}$ alloy) synthesized using the LDMD technique. In the future, the current authors will investigate further the effects of energy density during DED of NbTiNi samples.

Materials and methods

Elemental powders of pure nickel (99.7% Ni) and pure titanium (99.6%) were supplied by TLS Technik GmbH, and pure niobium (99.5% Nb) was supplied by Weartech (Pty) LTD. All three powders were spherical, having particle sizes ranging from + 45 µm to − 95 µm. It is known that spherical powder particles have good flowability and do not clog the nozzle during the LDMD process as compared to irregular powder [26, 27].

The powders were pre-mixed using a Tubular T2F mixer at 300 rpm for 12 h to achieve a homogenized mixture of $Ti_{51.25}Ni_{41.25}Nb_{7.5}$.

The deposition was done in a layer-by-layer manner using an IPG fiber laser. The GTV powder feeder was used to transport powder to a 3-way nozzle head attached to the KUKA robot arm.

Optimum laser process parameters that include laser power of 600W, laser scanning speed of 0.5 m/min, beam diameter of 2 mm, and shielding Argon gas of 15 l/min were used to fabricate 30 × 30 × 55 mm cube samples on a

Ti6Al4V base plate. The produced cube was wire machined to 8 × 4 × 4 mm rectangular samples for the heat treatment process and X-ray diffraction (XRD) characterization. For heat treatment, a carbolite furnace was heated at a rate of 10 °C/min to 700 °C and 900 °C, respectively, for 2 h, and the samples were furnace cooled.

Differential scanning calorimeter (DSC) DSC2A-02589, equipped with a cooling system (RCS90), was used to measure the phase transition temperatures. For DSC experimentation, microgram-sized shavings samples of about 6 mg in weight were used, and the samples were heated and cooled at a rate of 10 °C /min to determine the solid–solid-transition temperatures of the fabricated nitinol sample.

The as-built and heat-treated samples were metallographically prepared, surface polished to a mirror finish, etched with Kroll's reagent, and then characterized using Jeol JSM 6510 scanning electron microscope (SEM) with energy dispersive spectroscopy (EDS) and micro-Hardness (HV) using Zwick Vickers machine at a load of 500 g and dwell time of 10 s. XRD (XPERT PRO Analytical Netherland) that uses Cu kα radiation ($\lambda = 0.1545$ nm) set at voltage and current settings of 45 kV and 40 mA, respectively was used. X-ray patterns were scanned over a 2θ range from 10 to 90°. XPert and High score software were used to analyze the XRD patterns. The described process is summarized in Fig. 1.

Results and discussions

Figure 2 presents the microstructure and phase identity of the as-built and heat-treated samples.

SEM micrographs consisted of a dark phase rich in titanium, a light gray matrix that contains approximately 50–50 Ti–Ni plus Nb, and a whitish boundary rich in Nb. Figure 2b sample shows nucleation of dendrites, while Fig. 2c shows dendritic grain growth. It is known that dendritic growth in material affects mechanical properties.

The as-built in Fig. 2a shows a secondary lamella structure precipitate (NiTi and Nb) between the grains, which is the product of the pseudo-binary eutectic reaction of NiTi–Nb as proposed by Piao et al. [28]; this lamella precipitate suppressed the martensitic phase and Ti2Ni intermetallic which contributed in reducing the martensitic transition temperature [14]. However, after annealing, the β-Nb phase dissolves into the NiTi matrix, which is expected

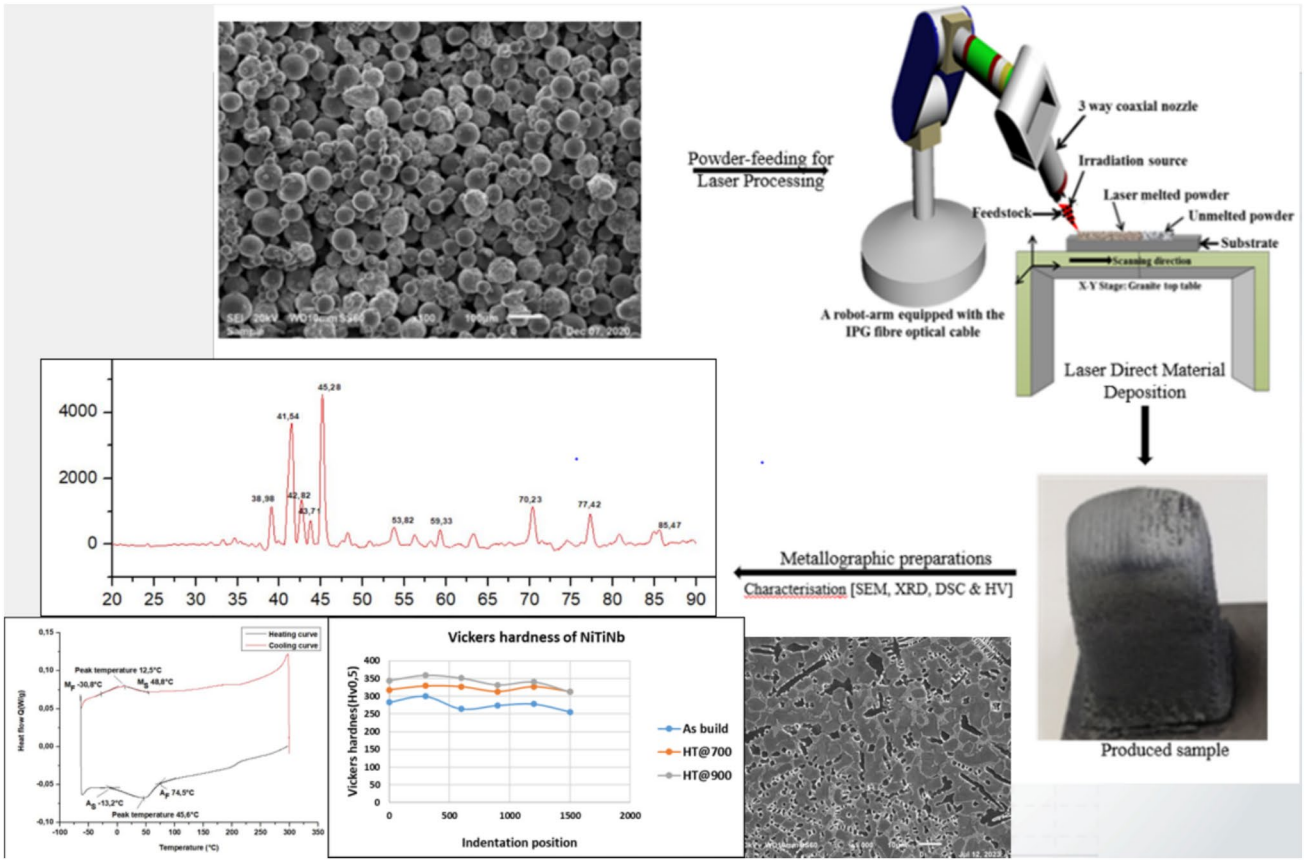

Fig. 1 Process set-up and sample characterization techniques

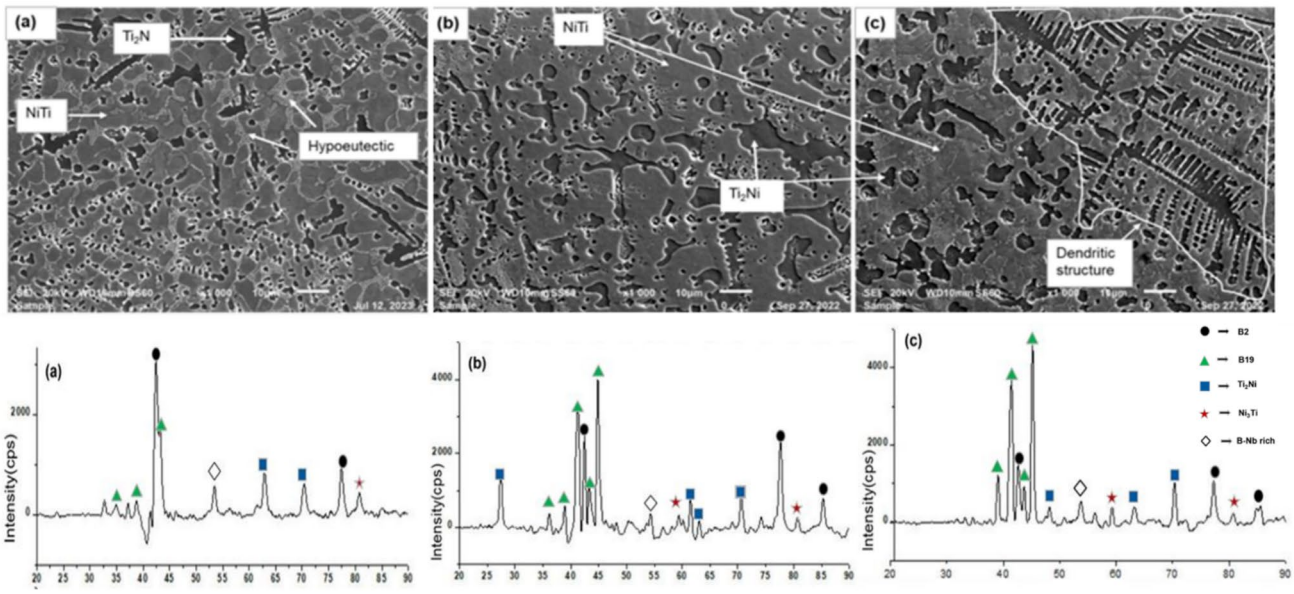

Fig. 2 Microstructure and XRD pattern graphs of the (**a**) As-built, (**b**) annealed at 700 °C, and (**c**) annealed at 900 °C samples

to affect martensitic transition temperatures and mechanical properties according to Fan et al. [18] and Wei et al. [19].

X-ray diffraction was used to determine the phases of the as-built and the heat-treated samples. Figure 2 shows the XRD patterns of the (a) as-built $Ti_{51.25}Ni_{41.25}Nb_{7.5}$, (b) sample annealed at 700 °C, and (c) sample annealed at 900 °C, respectively. The XRD patterns confirmed the presence of the Ti_2Ni, Ni_3Ti, β-Nb-rich, austenitic phase (B2), and martensitic phase(B19). An increase in the martensitic (B19) peak intensity was observed on both annealed samples (Fig. 2b, c) as compared to (Fig. 2a) as-built. There was also an increase in the proportion of Ni_3Ti identified with an increase in annealing temperature. It was assumed that annealing brings about oxidation of titanium, which reduces the ratio of Ni/Ti transitioning to Nickel-rich and leads to the formation of Ni_3Ti. Nucleation of brittle intermetallic (Ni_3Ti) into the matrix yields an increase in hardness.

Figure 3 represents the DSC scan results of NiTiNb alloy samples. Previous studies have indicated that the transition temperature changes of nitinol are sensitive to changes in the Ni/Ti ratio and/or the addition of a third element [8, 14, 26].

The DSC results in Fig. 3a–c show that the NiTiNb samples are hysteretic and reversible after annealing heat treatment. The sample annealed at 900 °C, Fig. 3c, shows an increase in the hysteresis temperature, while the hysteresis of the sample annealed at 700 °C slightly decreases. The hysteresis values calculated from (M_P–A_P) for the as-built, sample annealed at 700 °C, and the sample annealed at 900 °C are *33.1* °C, *29.8* °C, *and 36.16* °C respectively, and these hysteresis values are within typical hysteresis values of a binary Ni–Ti alloy which ranges between 20 and 50 °C [29].

The DSC also shows the increase in martensitic and austenitic transition temperature on both annealed samples, and this change is associated with the dissolution of Nb into the matrix and increased Ti_2Ni proportion.

Figure 4 presents the Vickers hardness results of the as-built and sample annealed at 700 °C and 900 °C NiTiNb synthesized via laser energy deposition.

The hardness results presented in Fig. 4 show higher hardness for samples annealed at 900 °C and lower hardness for both the as-built and samples annealed at 700 °C. Tracking back to the SEM micrographs observed in Fig. 2, annealed samples showed dendritic nucleation, dendritic growth, and an increase in Ti_2Ni; these features contribute to an increase in hardness according to the literature [4, 18]. Ti_2Ni intermetallic inhibits dislocation movement, leading to an increase in dislocation density that brings about a work-hardening effect. On the other hand, dendritic nucleation comes with an increase in hardness.

Conclusions

In this work, we investigated the effect of annealing heat treatment on microstructure, mechanical properties, and thermal properties of $Ti_{51.25}Ni_{41.25}Nb_{7.5}$ alloy fabricated using the LDMD process to enhance the mechanical and thermal properties.

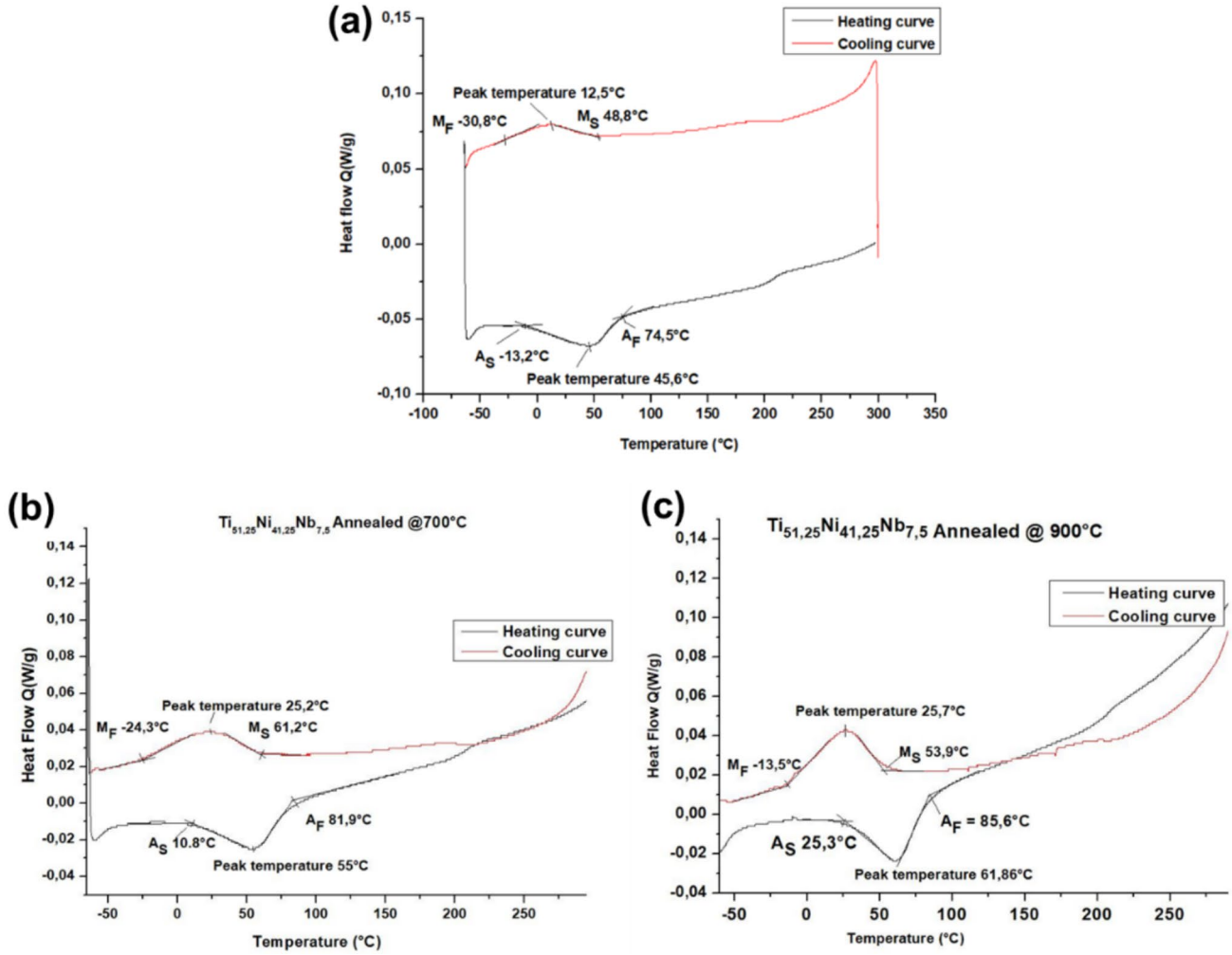

Fig. 3 Martensitic and austenitic thermal transition temperatures in NiTiNb alloy: (**a**) As-built, (**b**) annealed at 700 °C, and (**c**) annealed at 900 °C

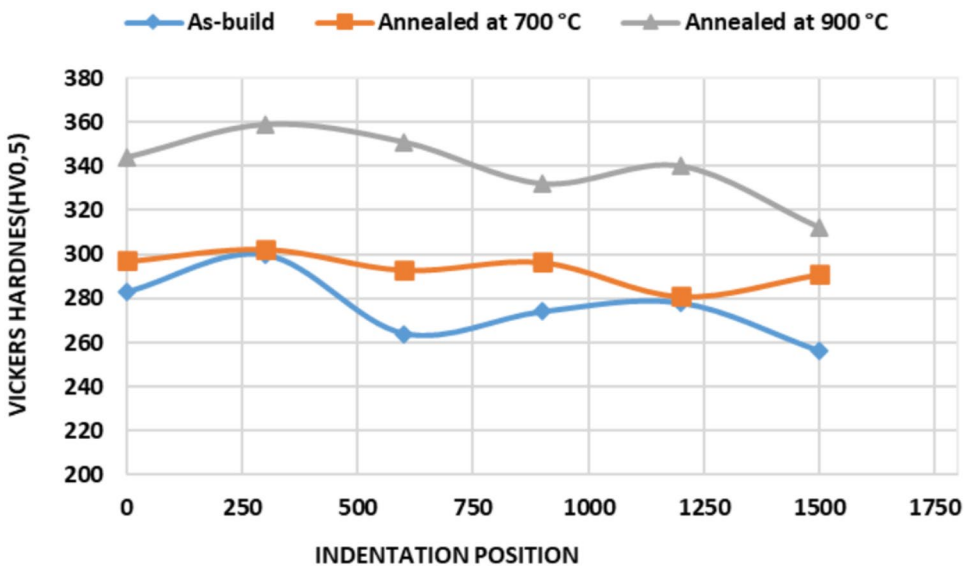

Fig. 4 The hardness of the as-built and heat-treated samples

- The eutectic structure observed on the as-built microstructure disappeared after annealing. It is assumed that it had dissolved into the matrix, which is the same observation of Xi et al. [25].
- The annealing heat treatment performed at 900 °C realized microstructural changes that yielded an increase in Ti_2Ni intermetallic proportion, which caused an increase in the hardness of NiTiNb samples produced by the LDMD process, while annealing performed at 700 °C has homogenized the hardness.
- Annealing of NiTiNb increased both the martensitic and austenitic transition temperatures. The sample annealed at 900 °C reported slightly higher hysteresis than the sample annealed at 700 °C, which impacts the shape memory effect and superelasticity. We agree with Nie et al. [30] that an investigation of the effect of heat treatment on superelasticity and SME is needed for future work.
- XRD patterns confirmed the presence B19, B2, Ti_2Ni, Ni_3Ti, and β-Nb-rich, and it also confirms increase in Ni_3Ti with increase in annealing temperature.

Acknowledgments The authors would like to thank the Council for Scientific and Industrial Research (CSIR) for the facilities used to conduct this research, the National Research Foundation (NRF), and the African Laser Centre (ALC) for their funding contribution to this study.

Author contribution All authors contributed to the study's conception and design. Material preparation and data collection were performed by [Mr. Samuel Skhosane] and [Paul Lekoadi], while data analysis was performed by [Samuel Skhosane], [Prof Nthabiseng Maledi], [Prof Sisa Pityana], [Dr. Monnamme Tlotleng], and [Mr. Paul Lekoadi]. The first draft of the manuscript was written by [Samuel Skhosane], and all authors commented on previous versions of the manuscript. All authors read and approved of the final manuscript.

Funding Open access funding provided by Council for Scientific and Industrial Research. This work was supported by the National Research Foundation (NRF) grant No: TTK230509104124, and Partial financial support was received from the African Laser Center (ALC) grant No: HLHA25X task ALC-R008.

Data availability Data will be available on reasonable request.

Declarations

Conflict of interest The authors declare that they have no conflict of interest.

References

1. M.N. Mokgalaka, S.L. Pityana, P.A.I. Popoola, T. Mathebula, Adv. Mater. Sci. Eng. **214**, 363917 (2014)
2. J.C. Chekotu, R. Groarke, K. O'Toole, D. Brabazon, Mater. **12**(5), 809 (2019)
3. J.W. Mwangi, L.T. Nguyen, V.D. Bui, T. Berger, H. Zeidler, A. Schubert, J. Manuf. Process. **38**, 355–369 (2019)
4. I. Polozov, A. Popovich, Mater **14**, 2696 (2021)
5. P. Jamshidi, C. Panwisawas, E. Langi, S. Cox, J. Feng, L. Zhao, M. Attallah, J. Alloy. Compd. **909**, 164681 (2022)
6. P. Halani, I. Kaya, Y. Shin, H. Karaca, Mater. Sci. Eng. A **559**, 836 (2013)
7. R. Zhu, G. Tang, S. Shi, M. Fu, J. Mater. Process. Technol. **1**, 30 (2013)
8. P. Šittner, L. Heller, J.C. Pilch, T. Alonso, D. Favier, J. Mater. Eng. Perform. **23**, 2302 (2014)
9. T. Odaira, S. Xu, K. Hirata, X. Xu, T. Omori, K. Ueki, K. Ueda, T. Narushima, M. Nagasako, S. Harjo, T. Kawasaki, Adv. Mater. **34**(27), 2202305 (2022)
10. H. Huang, H. Zheng, G. Lim, G. Appl, Surf. Sci. **228**, 201 (2004)
11. B.S. Skhosane, M. Tlotleng, S. Pityana, MRS Adv. **5**, 23 (2020)
12. C. Ying, J. Hai-Chang, R. Li-Jian, X. Li, Z. Xin-Qing, Intermetallic. **19**, 271 (2011)
13. Y. Li, F. Zhang, T.T. Zhao, M. Tang, Y. Liu, Rare Met. **33**, 244 (2014)
14. D. Cascadan, C. Grandini, In Recent Adv. Metall. Eng and ED. 1 (2019)
15. H. Shi, S. Pourbabak, J. Humbeeck, D. Schryvers, Scr. Mater. **67**, 939 (2012)
16. M.E. Cronemberger, V.H. Menezes, R.D. Silva, I.G. Santos, V.L. Sordi, S.E. Kuri, C.A. Rovere, Mater. Res. **22**, (2019)
17. J. Van Humbeeck, Le Journal de Physique. **7**, 5 (1997)
18. Q. Fan, Y. Zhang, Y. Zhang, Y. Wang, E. Yan, S. Huang, Y. Wen, J. Alloys Compd. **790**, 1167 (2019)
19. L. Wei, Z. Xinqing, Chin. J. Aeronaut. **22**, 540 (2009)
20. V. Sharma, D. Svetlizky, M. Das, O. Tevet, M. Krämer, S. Kim, B. Gault, N. Eliaz, Addit. Manuf.. Manuf. **86**, 104224 (2024)
21. P. Ghosal, M. Majumder, A. Chattopadhyay, Mater. Today Proc. **5**(5), 12509–12518 (2018)
22. A. Attaran, Bus. Horiz.Horiz. **60**(5), 677–688 (2017)
23. S. Kumar, L. Marandi, V. Balla, S. Bysakh, D. Piorunek, G. Eggeler, I. Sen, Mater. **8**, 100456 (2019)
24. F. Zhang, L. Zheng, F. Wang, H. Zhang, J. Alloys Compd. **735**, 2453 (2018)
25. R. Xi, H. Jiang, G. Li, Z. Zhang, H. Wei, G. Zhao, J. Van Humbeeck, X. Wang, Int. J. Extreme Manuf. **6**(4), 045002 (2024)
26. L. Liu, I. Marziano, A. Bentham, J. Litster, E. White, T. Howes, Int. J. Pharm. **362**, 109 (2008)
27. D. Boisselier, S. Sankaré, Phys. Procedia **39**, 455 (2012)
28. M. Piao, S. Miyazaki, K. Otsuka, N. Nishida, Mater. Trans. **33**, 337 (1992)
29. C. Slough. TA. Instrum. 1–5 (2007)
30. M. Nie, P. Jiang, X. Li, D. Zhu, T. Yue, Z. Zhang, Surf. Coat. Technol. **487**, 131020 (2024)